

# 成都理工大学核技术与自动化工程学院 首届研究生学术研讨会论文集

Proceeding of the First Graduate Technicality Symposium of College of Nuclear  
Technology and Automation Engineering at CDUT



穷究于理 成就于工

成都理工大学核技术与自动化工程学院  
College of Nuclear Technology and Automation Engineering

四川·成都  
二〇〇五年十二月

# 成都理工大学核技术与自动化工程学院 首届研究生学术研讨会论文集

Proceeding of the First Graduate Technicality Symposium of College of  
Nuclear Technology and Automation Engineering at CDUT

2005. 12

江苏工业学院图书馆  
藏书章

成都理工大学核技术与自动化工程学院研究生会

四川·成都



## 前 言

随着我国科教兴国战略的实施以及高等教育的普及，越来越多的人能够接受研究生教育。随着研究生招生规模的扩大，如何在增加研究生培养数量的同时，提高研究生人才的培养质量，是我国研究生教育及社会关注的热点。

核技术与自动化工程学院研究生会精心组织的“成都理工大学核技术与自动化工程学院首届研究生学术研讨会”顺利召开了。会议收到论文 32 篇，并择优编辑成论文集。涵盖了核技术及应用、地球化学、计算机应用、自动化控制等领域。此次研讨会为广大研究生提供了一个交流信息、总结经验、共同进步的平台；促进了我院各学科各领域内的交流与合作，大大活跃了学术氛围；对于提高研究生论文撰写、科研报告及演讲能力起到了非常重要的作用。

这部学术论文集既是对过去研究生工作的总结与肯定，也是对今后研究生教育的勉励。希望每一位来到核技术与自动化工程学院学习的研究生都学有所长，成为建设中国特色社会主义的栋梁之才，为中华民族的伟大复兴做贡献。

感谢成都理工大学研究生院对本次研讨会的大力支持，对精心培养研究生的各位导师表示崇高敬意，感谢研究生会的全体同学，他们为研讨会的顺利召开付出了辛勤的努力。

元旦将至，新的一年即将来临，在此祝愿各位工作顺利、新年愉快！

葛良全

2005年12月 成都

# 目 录

## 国际会议论文-----

POCKET POWER SUPPLY SYSTEM FOR SI-PIN DETECTOR.....	林延畅,姜海静,葛良全,赖万昌,程锋(1)
PATTERNS OF ATMOSPHERIC DUST TRACE HEAVY METAL ELEMENT CONCENTRATIONS IN CHENGDU, CHINA .....	陈敏,张成江,倪师军,施泽明(5)

## 核技术及其应用-----

XRF 法快速测定铁钛精矿中 FE、TI 品位.....	郭生良,赖万昌,程锋,郭伟(10)
X- $\Gamma$ 吸收剂量率检测仪显示电路的研究 .....	崔妍,侯新生(13)
X 射线荧光技术在新疆某航磁异常地面勘察的应用 .....	花永涛,赖万昌,杨强,程锋(18)
半导体致冷原理及其应用系统设计研究.....	郑永明,方方,徐建一,郑燕红(23)
便携式瞬时土壤测氦仪的研制 .....	王玉双,葛良全,姜海静(28)
成都某区域环境氡水平调查 .....	李丹,葛良全,田丽霞,杨强(32)
基于 MAPOBJECTS 的核勘查数据处理系统.....	殷文娟,马英杰,周蓉生(37)
建筑材料中的氡析出率研究 .....	谢斐,童菡茵,刘晓辉,杨强(42)
扩散式环境测氦仪器的研制 .....	郑奕挺,王晓丹,方方,周蓉生(47)
小型氡室系统的实验研究 .....	王敏,吴婷,张国华(52)
一种电荷灵敏前置放大器的研制 .....	耿波,周程,方方,张国华,郑奕挺(58)
一种新型电离室 $\alpha$ 测氦仪的研制 .....	张国华,赵为松,王敏(62)

## 地球化学-----

GPS 滑坡监测系统在铁路桥桥墩稳定性监测中的应用 .....	吕军,周蓉生,侯新生(66)
地气测量研究河床中的断裂构造 .....	郭伟,童纯菡,刘晓辉,郭生良(70)
广西玻璃陨石微量元素区域分布聚类分析 .....	喻凤莲,张成江,倪师军,陈敏(74)
冀北赤城退变榴辉岩的岩石地球化学及其原岩恢复.....	周兵,倪志耀,张成江,倪师军(78)
流动注射化学发光法测定 CO(II) .....	庞雪华,张成江,倪师军(83)
中低放废物地质处置方法 .....	周晓剑,张成江,倪师军(87)

## 自动化控制与应用-----

地坑升降机设计 .....	高超,肖鹏,郭伟,郭生良(92)
基于 I—WIRE 总线的智能多点测温系统设计 .....	李金凤,吴建平(97)
基于 EPP 协议的虚拟数据采集与分析系统 .....	杨强,赖万昌,花永涛,王广西(102)
基于 FPGA 的 PCMCIA 接口桥设计 .....	吴婷,王敏,周程(107)
基于 MATLAB6.5 路径追踪控制器控制效果仿真 .....	周丹,李宏穆(112)
基于 USB 技术的人机接口类的应用 .....	周程,耿波,吴婷(116)
基于 VISUAL BASIC 开发的传感器微机测试系统 .....	吴春蓉,吴建平(119)
基于凌阳 SPCE061A 控制的语音玩具小车的实现 .....	沈立,周四春,杨伟涛(124)
液晶显示模块 QH2001 及其在核仪器中应用 .....	赵为松,张国华,方方(129)

# Pocket Power Supply System for Si-PIN Detector<sup>\*</sup>

LIN Yan-chang, JIANG Hai-jing, GE Liang-quan, LAI Wan-chang, CHENG Feng

( College of Nuclear Technology and Automation Engineering, Chengdu University of Technology, 610059, China. )

**Abstracts:** A high efficiency power supply system for thermoelectrically cooled Si-PIN detector, which fits in a shirt pocket, was designed and introduced in this paper. Idea about Pulse Width Modulation (PWM) based pre-amplifier power supply, PWM based self-adjustable voltage regulator for electric cooler, and a charge pump based transformerless low ripple noise high voltage bias for Si-PIN detector was carried out. More electronic techniques are applied in the system so that smaller dimension, less power consumption and higher reliability should be achieved. As the performance of high voltage bias is important for the whole detector system. The new design was test under condition of  $-5^{\circ}\text{C}$  up to  $43^{\circ}\text{C}$ . And the high voltage output ranges from 100.85V to 100.32V, while maximum ripple noise is less than 15mV. The system can be widely adopted in various In-situ X-Ray Fluorescence spectrometry based on Si-PIN detector.

**Key words:** In-situ XRF; Si-PIN detector; PWM; charge pump; ripple noise; reliability

## Introduction

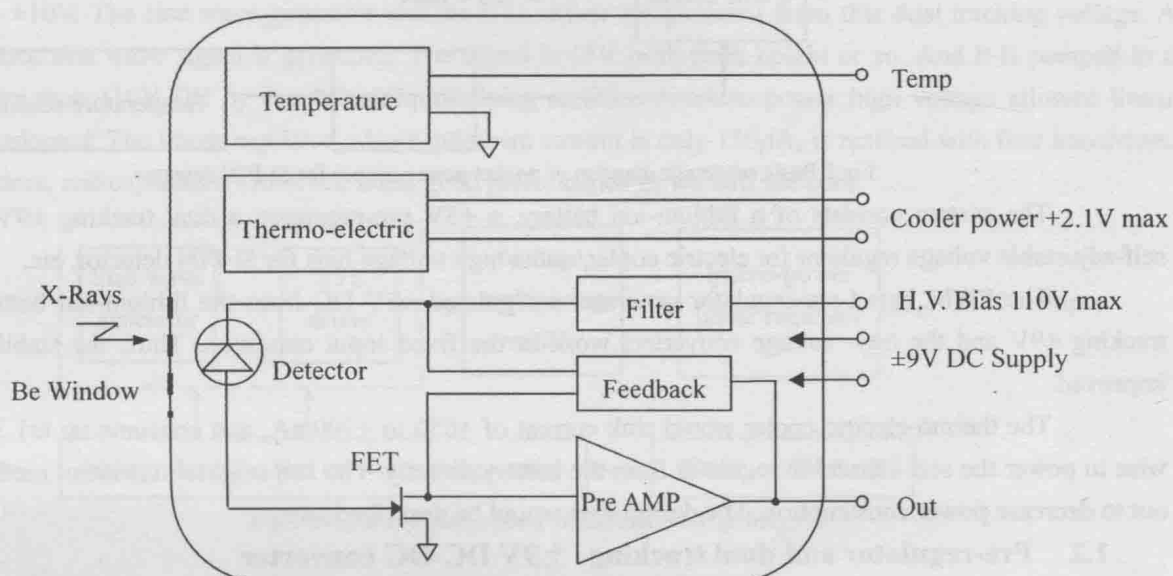


Fig.1 Internal configuration of Si-PIN detector (model XR-100CR)

In-situ X-Ray Fluorescence (XRF) sampling techniques are widely use in various regions, such as geoscience, mineralogy, archaeology and astronomy, etc <sup>[1]</sup>. The performance of Portable X-Ray Fluorescence (PXRF) spectrometry increases along with the development of science and technology. High energy resolution XRF tele-data-acquisition on Mars was realized <sup>[2]</sup>(Principally refer to the invention of Si-PIN detector for X-Ray detection).

The internal configuration of Si-PIN detector (model XR-100CR), from Amptek, INC., is shown in fig.1. It requires a dual tracking  $\pm 9\text{VDC}$ , a  $+2.1\text{V}$  max DC cooler power and a  $+110\text{V}$  max detector bias. Nowadays, more and more such detectors are adopted in PXRF spectrometry. Since the special power supply and shaper amplifier (model PX2CR) can't work in field without AC power. Designing a battery powered supply system with small dimension, high efficiency and well reliability is extremely critical.

<sup>\*</sup> Supported by the National Science Foundation of China (40274048, 40374051) and the Youth Science Foundation of Chengdu University of Technology (2004QJ21).

<sup>\*</sup> Collected by Paper Collection of International radiation physics society workshop on frontier research in radiation physics and related areas, Nov. 2004.

A Si-PIN X-Ray detector based PXRF spectrometry for geologic survey, Model IED-2000P, was successfully designed in Chengdu University of Technology (CDUT) in 1999<sup>[4]</sup>. Some other study on practically techniques for In-situ XRF sampling, and some relative electronic units as well, is supported by the National Science Foundation of China (40274048, 40374051) and the Youth Science Foundation of CDUT (2004QJ21). Here's some application hints for Si-PIN detector power supply designing, which were obtained in the study.

## Schematic diagram

### 1.1 Basic schematic diagram

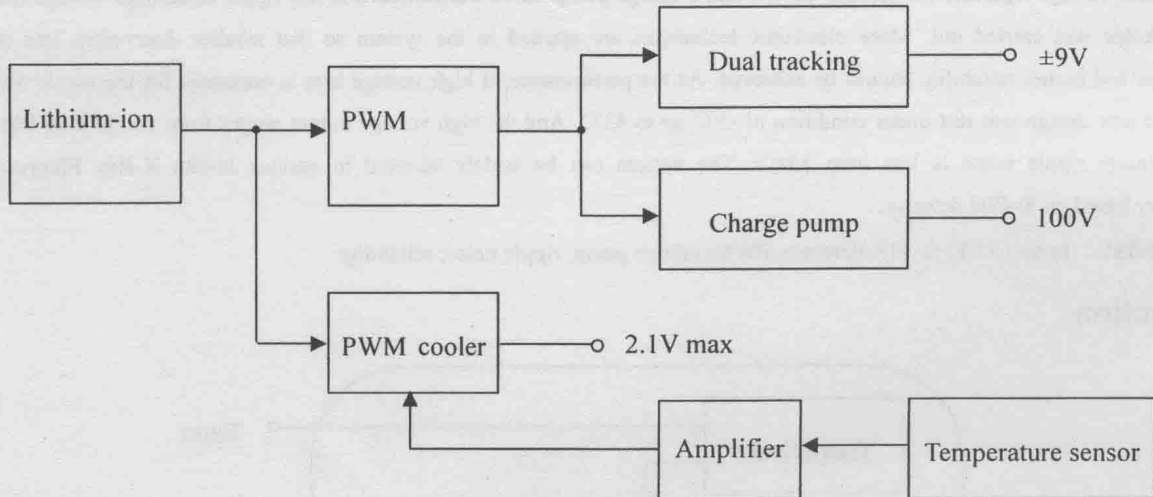


Fig.2 Basic schematic diagram of pocket power supply for Si-PIN detector

The system consists of a lithium-ion battery, a +5V pre-regulator, a dual tracking  $\pm 9V$  converter, a self-adjustable voltage regulator for electric cooler, and a high voltage bias for Si-PIN detector, etc.

The PWM based pre-regulator generates a regulated +5V DC from the lithium-ion battery. The dual tracking  $\pm 9V$  and the high voltage converters work in the fixed input condition. Thus, the stability would be improved.

The thermo-electric cooler would sink current of +650 to +700mA, and consume up to 1.3W or so. It's wise to power the self-adjustable regulator from the battery directly. The self-adjustable control method is carried out to decrease power consumption. The design idea would be described later.

### 1.2 Pre-regulator and dual tracking $\pm 9V$ DC-DC converter

The MAX1687 step-up DC-DC converter provides over 90% conversion efficiency. The device can provide a +5V output with high current burst ability from a single Lithium-ion cell. It is idea for the application of pre-regulator. The typical operating circuit provided in the device datasheet works well. Hence, no more description is necessary.

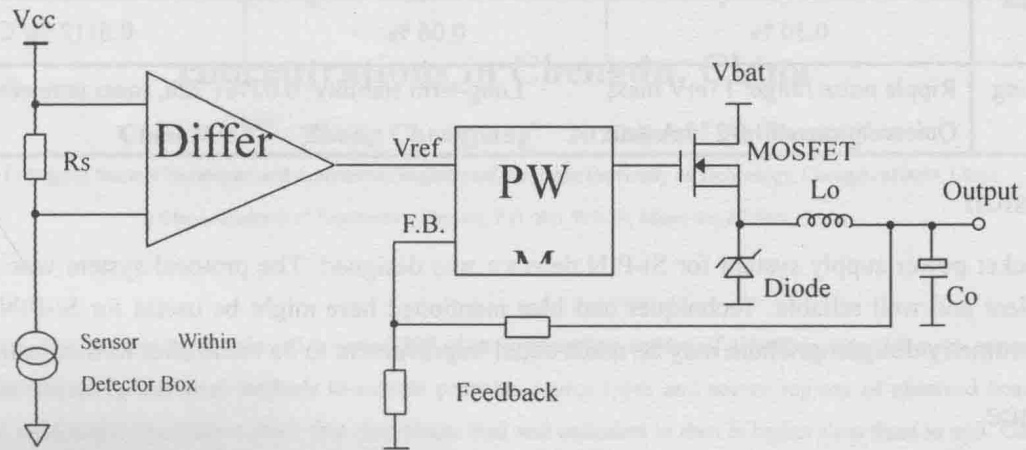
The dual tracking DC-DC converter is based on the device MAX743. For the device is designed to provide  $\pm 12V$  or  $\pm 15V$  from a single +5V input voltage, some treatment should be done to make the device supports  $\pm 9V$  output directly. Two resistors could be paralleled with each internal feedback resistors to change the feedback factor. The optional Pi filters should be used to decrease the level of ripple noise.

### 1.3 PWM based self-adjustable voltage regulator for electric cooler

Once the temperature gets below  $-10^{\circ}C$ , the performance of the XR-100CR system will not change with a temperature variation of a few degrees. Hence, accurate temperature control is not necessary<sup>[2]</sup>. Nevertheless, negative feedback should be adopted in a battery-powered system. Along with the decreasing of temperature, the regulator should self-adjust the output voltage to a lower level to decrease power consumption.

The configuration of the self-adjustable voltage regulator for electric cooler is offered in fig.3. Where the output voltage of the amplifier, which is proportional to the temperature of the detector, acts as the reference

voltage  $V_{ref}$  for the PWM controller and adjusts the output of the whole regulator. The diode should be fast



recovery type. This output voltage can ranges from 1.5V to 2.1V corresponds to  $-30^{\circ}\text{C}$  up to  $70^{\circ}\text{C}$ .

Fig.3 schematic diagram of self-adjustable voltage regulator for electric cooler

1.4 Charge pump based transformerless low ripple noise high voltage bias

Refer to fig.4, the single chip voltage doubling and inverting charge pump converts the +5V input voltage into  $\pm 10\text{V}$ . The sine wave generator and the BTL driver are powered from this dual tracking voltage. A low impedance sine wave signal is generated. The signal is 17V peak-peak height or so. And it is pumped to a level of more than 110V DC by the voltage multiplying rectifier. A micro-power high voltage allowed linear regulator is adopted. The linear regulator, whose quiescent current is only  $150\mu\text{A}$ , is realized with four transistors, several resistors, and capacitors. However, it has good performance as we will see soon.

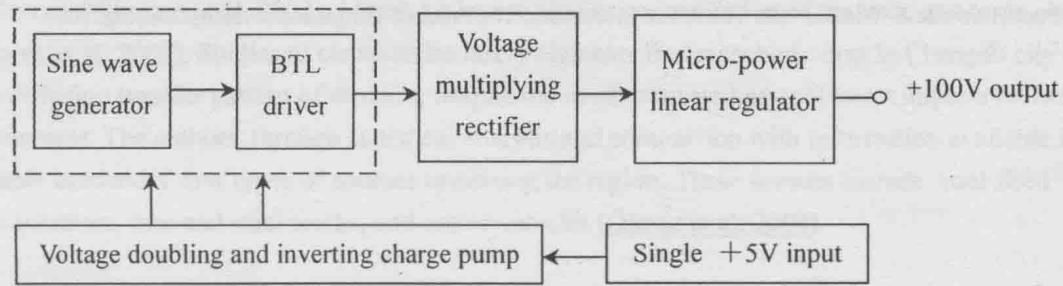


Fig.4 Diagram of charge pump based high voltage bias

System testing

A protocol system is made. Most of the components are in SMT package. The whole system is finally housed in a box sizing  $100\times 60\times 25\text{ mm}^3$ . It fits in a shirt pocket.

As the designing purpose, the circuit of pre-regulator, the dual tracking converter, and the self-adjustable regulator works well. For shortage of time, only the high voltage bias for detector has been tested detailedly by now. Some testing data and results are list in table.1. As the real world detector would sink  $10\mu\text{A}$  from the bias. An equivalent resistance load of  $10\text{M}\Omega$  was used except load regulation testing.

Table.1 Testing data and results of charge pump based high voltage bias

Testing condition and original data	Output voltage vs. load current		Output voltage vs. input voltage		Output voltage vs. air temperature	
	0 $\mu\text{A}$	100.79 V	4.5 V	100.72 V	-5 $^{\circ}\text{C}$	100.85 V
	10 $\mu\text{A}$	100.77 V	5 V	100.76 V	12 $^{\circ}\text{C}$	100.79 V
	50 $\mu\text{A}$	100.69 V	6 V	100.77 V	14 $^{\circ}\text{C}$	100.77 V
	100 $\mu\text{A}$	100.49 V	7 V	100.78 V	43 $^{\circ}\text{C}$	100.32 V



Results based on the data above	Load regulation	Voltage regulation	Temperature coefficient
	0.30 %	0.06 %	0.0112 %/°C
Other testing results	Ripple noise range: 15mV max; Quiescent current: 27mA max; Long-term stability: 0.02% ( 72h, room temperature).		

Conclusion

A pocket power supply system for Si-PIN detector was designed. The protocol system was found out to be high efficient and well reliable. Techniques and idea mentioned here might be useful for Si-PIN detector based XRF spectrometry designing. There may be much detail improvement to be made after further testing.

Reference

[1].GE Liang-quan, ZHOU Si-chun, LAI Wan-chang. In-situ X Radiation Sampling Technique. The Press of Science and Technology of Sichun. Chengdu, 1997.

[2].Operating Manual XR-100CR X-Ray Detector System and PX2CR Power Supply/Shaper. Amptek Inc. U.S.A.

[3].JIANG Hai-jing, LIN Yan-chang, GE Liang-quan, et al. Transformerless high voltage Bias for Si-PIN detector. Nuclear Electronics & Detection Technology, 2004, Vol.24 (6): 711-713.

[4].LAI Wan-chang, GE Liang-quan, WU Yong-peng, et al. Research and application of a sensitive XRF analyzer based on Si-PIN detector. Nuclear Techniques, 2003, Vol.26(11): 891-895.

[5].LIN Yan-chang, GE Liang-quan, LAI Wan-chang. The Application of portable multi-element XRF analyzer to geological survey. Geophysical & Geochemical Exploration, 2003, Vol.26(4): 325-328.

[6].Paul Horowitz & Winfied Hill. The Art of Electronics. The Press of Tsinghua University. Beijing, 2003.



# Patterns of atmospheric dust trace heavy metal element concentrations in Chengdu, China

Chen Min<sup>a,b\*</sup> Zhang Chengjiang<sup>a</sup> Ni Shijun<sup>a</sup> Shi Zeming<sup>a</sup>

<sup>a</sup> College of Nuclear Techniques and Automation Engineering, Chengdu University of Technology, Chengdu 610059, China

<sup>b</sup> China Academy of Engineering Physics, P.O. Box 919-71, Mianyang 621900, China

## Abstract

Atmospheric dust sample were selected in over 300 sites surrounding center of Chengdu city. Element concentrations of samples were determined by chemical methods to explain probable source types and source regions of observed heavy elements. Ratio of element pairs and concentration show that chromium, lead and cadmium in dust is higher than them in soil. Concentrations for the elements displayed that were effected by industries.

*Keywords:* atmospheric dust; element; metal; China

## Introduction

Heavy metal elements have been determined in atmosphere dust for several decades and for variety of reasons. Some have gone so far as to suggest that certain geographical areas have such strong sources of various elements that they have unique regional emission patterns that can be used to distinguish the contribution of the different regions at distant receptor locations. Z.G. Guo studies elemental and organic characteristics of dust in Qingdao, China (Guo et al. 2004). Nikolaos S. Thomaidis characterizes some heavy metal element in atmosphere in Greece (Nikolaos et al. 2003). Marek Lisiewicz studies concentration of the toxic and toxic element in door dust (Marek et al. 2000). Studies to characterize heavy elements in atmospheric dust in Chengdu city can help understand diffusion transfer pattern of element, despite the need to assess heavy element impacts on human health and environment. The authors, through statistical analysis and comparison with information available in the literature, were able to identify four types of sources impacting the region. These sources include: coal-fired power plants, incinerators, iron and steel works, and motor vehicles (Ölmez et al. 2004).

The Sichuan Basin is a fertile, subtropical expanse of low hills and plains completely encircled by mountains. Temperatures in the Sichuan Basin are mild with very warm summers (26 to 29°C) and cool winters (5 to 8°C). Mountains to the north of the basin moderate winter cold by blocking the southward movement of cold air from Central Asia. Because the climate is humid and surrounding mountains impede air circulation, the Sichuan Basin is prone to temperature inversions. Summers are often overcast or very hazy and fog is present many days during the winter. Climate for Chengdu is typical of cities located on high upland plateaus: the rage between summer and winter temperatures is extreme, so appropriate seasonal clothing is strongly advised. In fact, Chengdu locating in the western part of the Sichuan Basin averages more than 300 days a year of foggy weather. The objective of this study was to collect and analyze dust samples for Chengdu city and explain probable source types and source regions for observed heavy element concentrations. 305 sampling sites were selected from center of city to outside of highway surrounding city (see Fig.1). In fact, sampling zone includes that longitude of sampling zone is from E103.9389° to E104.2026°, and latitude of it is from N30.56369° to N30.75028°.

\* Corresponding Author, Cheng Min, Tel:+86-2866834807, E-mail address: cm907@126.com

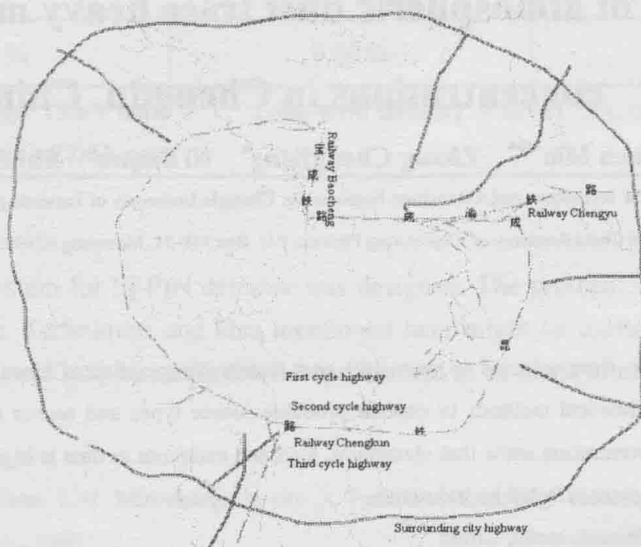


Fig.1 Atmosphere dust sampling zone in Chengdu, China

## Experimental

Samples of old atmosphere dust are collect by brush from wall, window and door which aren't coated any paint. In every sampling site mass of collecting dust sample is over 100g. The collected samples were packaged small zip-lock polyethylene bags. All measurement is finished by Sichuan Analytical and Testing Center for Mining. The concentration of element were determined such as Hg, Cd, As, Cr, Pb, Cu, Zn, Ni, Al, Ca, Co, Fe, K, Mg, Mn, Na, S, P, Si, Ti, V, and so on. Samples were determined by ICP-MS and electrochemical method. Analytical results were compared with certified values.

During collecting sample, GPS is used to record the position. In this work, GIS is used to locate sampling site in city and find neighbor industries and company, etc., which is the Statewide Chinese Map ([Map Center of China, 2005](#)).

## Results and Discussion

Comparing with ratio of special elements can help obtain information about diffusion transfer of element. The authors have confirmed some ratio between special elements in soil. The ratio of element pairs was applied to confirm the origin of obsidian sample ([Almzán-Torres et al. 2004](#)). Table 1 summarizes the results of elementary ratio in dust and them in soil which given by other authors ([Liu et al. 1984](#); [Xing et al. 2003](#)). It shows that concentration of chromium rises from data of V/Cr and Mn/Cr. Meanwhile, concentration of lead and cadmium rises, too. In general, there is distinct difference elementary ratio between dust and soil. Data in table 2 confirm it, too. Concentration of chromium, lead and cadmium in dust are higher than them in soil. It shows that there are extrinsic sources.

Table 1. Elementary ratio in dust and soil ( $\mu\text{g/g}$ )

Element pair	Ratio in soil (R, SD)	Ratio in dust (R, SD)
V/Cr	1.6 $\pm$ 0.63	0.48 $\pm$ 0.21
Ni/Co	2.29 $\pm$ 0.75	20.88 $\pm$ 6.84
Mn/Cr	8.86 $\pm$ 5.39	6.63 $\pm$ 4.03
Zn/Cu	3.48 $\pm$ 1.55	4.96 $\pm$ 2.21
Zn/Pb	3.65 $\pm$ 1.55	3.04 $\pm$ 1.29
Zn/Cd	641 $\pm$ 346	276 $\pm$ 149

Table 2. Elementary concentration in dust and soil for Chengdu ( $\mu\text{g/g}$ )

Element	Concentration in dust			Concentration in soil(Zhu et al. 2004)		
	min	max	average	min	max	average
Cr	18.98	647.08	111.98	17.900	145.000	79.454
Pb	119.76	1327.42	372.01	21.00	311.00	50.768
Cd	0.17	20.80	4.33	0.100	0.710	0.2116

For acquainting with pollution distribution of heavy trace element, concentration of elements is summarized as from fig.2 to fig.4 and color bar is used to show its concentration. Meanwhile, sites whose concentration is more half than the average are drawn another on right side so that can help to recognize distribution of trace heavy metal element. Fig.2 shows that main pollution sites by chromium distributes from southeast to northeast. There are zone with high concentration of chromium closing the second cycle highway (see fig.2C). In fact, the site with high concentration of chromium is close a leather company. Of course, confirming pollution source need more work.

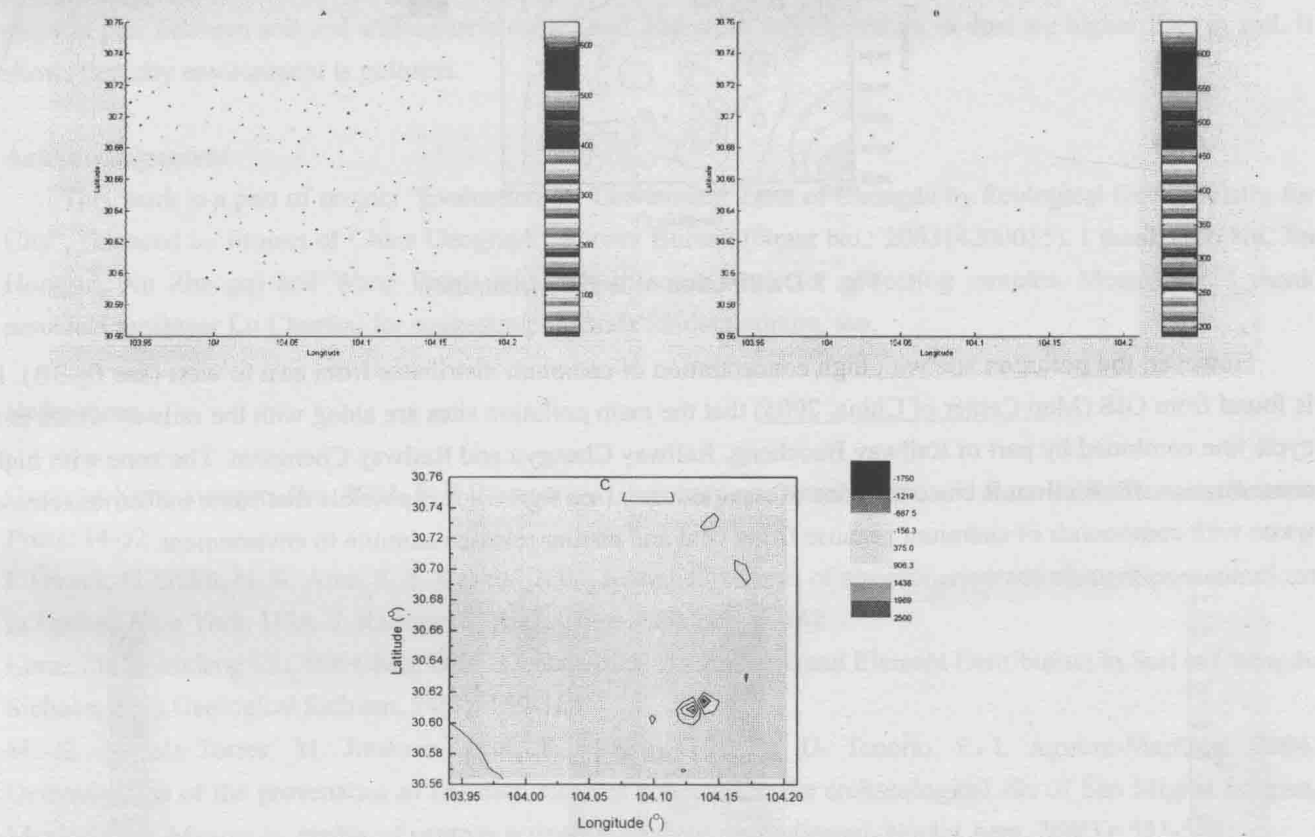


Fig. 2 Distribution of chromium concentration

The pollution site with high concentration of lead distributes from southeast to northeast, too (see fig.3B). Then there are some distinct pollution sites in the northeast corner of city. The main pollution sites are along with the highway such as Road Wuhou, the third cycle highway, and so on, especially in the southwest of the third cycle highway (see fig.3C). It shows that the main source is traffic tools because lead adds in gasoline. Therefore, the time of gasoline added compounds of lead need stop.

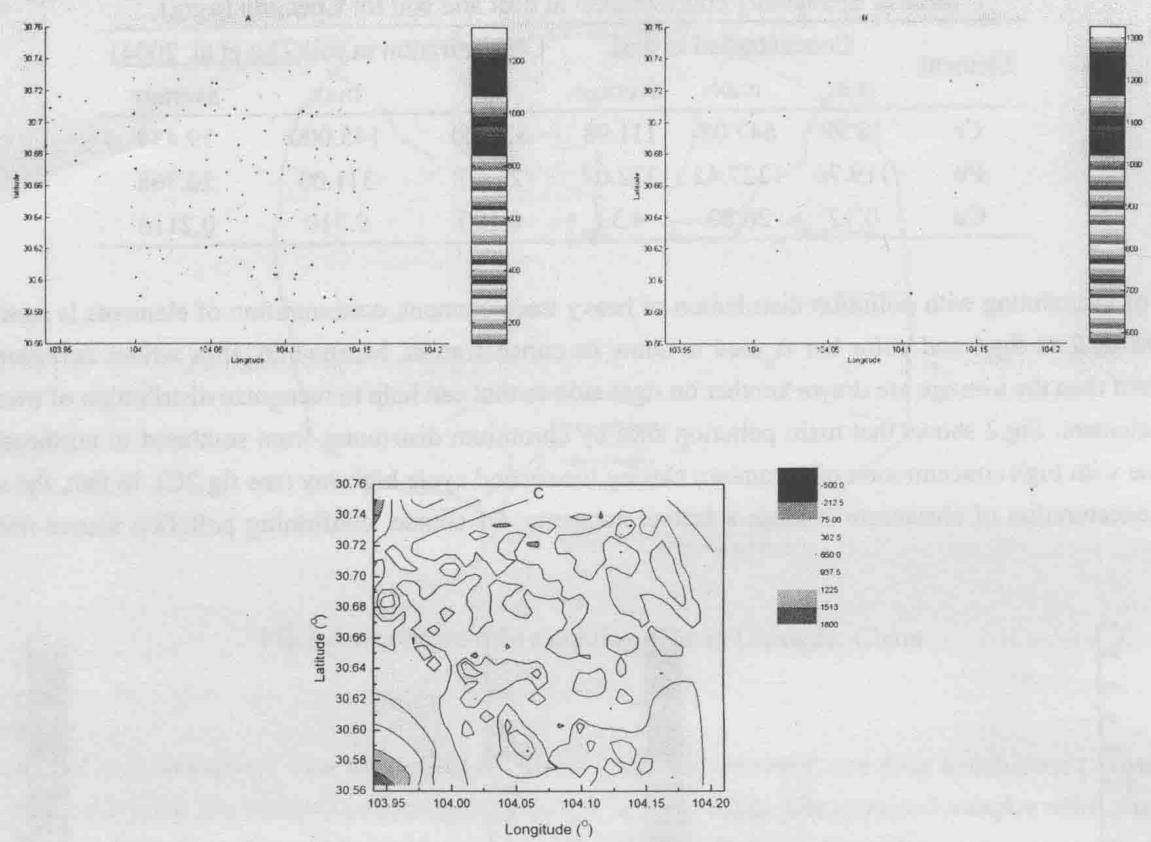
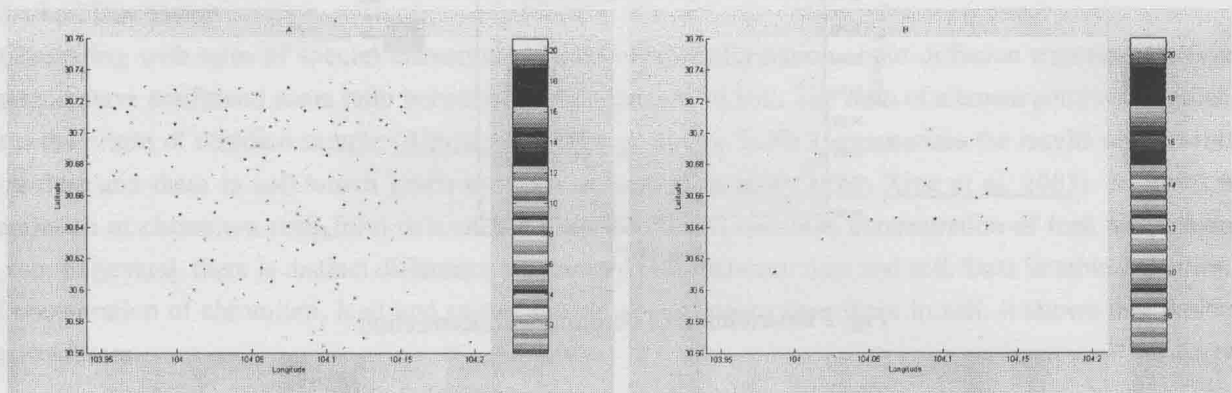


Fig. 3 Distribution of lead concentration

However, the pollution site with high concentration of cadmium distributes from east to west (see fig.3B). It is found from GIS (Map Center of China, 2005) that the main pollution sites are along with the railway which is a cycle line combined by part of Railway Baocheng, Railway Chengyu and Railway Chengkun. The zone with high concentration of cadmium is close the zone of steel industry (see fig.4C). It is possible that some industries release waste with compounds of cadmium because firing coal and plating release cadmium to environment.





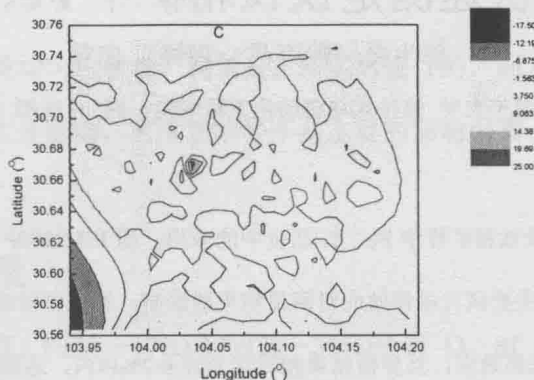


Fig. 4 Distribution of cadmium concentration

### Conclusions

There are different distribution patterns for different element. However, all of them are results which human's action affects environment, especially, industries and traffic. There is obviously difference for the ratio between element pair between soil and atmospheric dust. Lead, cadmium and chromium in dust are higher than in soil. It shows that city environment is polluted.

### Acknowledgement

This work is a part of project "Evaluation for Economical Zone of Chengdu by Ecological Geochemistry for City", financed by Project of China Geography Survey Bureau (Grant No.: 200314200015). I thank Guo Hu, Jin Hongrui, Xu Zhengqi and Wang Pingli take part in some work for collecting samples. Meanwhile, I thank associate professor Lu Chunhai for suggesting methods for data mining, too.

### References

- Guangxi Xing, Jianguo Zhu. 2003. Soil Elementary Chemistry on microelement and Rare Earth Element. Science Press: 14-32
- I. Ölmez, G. Güllü, N. K. Aras, S. S. Keskin. 2004. Seasonal patterns of atmospheric trace element concentrations in Upstate New York, USA. *J. Radioanal. Nucl. Chem.* 259(2): 157-162
- Lixue Zhu, Zhixiang Liu, Bin Chen. 2004. Geochemical Background and Element Distribution in Soil in Chengdu, Sichuan. *Acta Geological Sichuan.* 24(3): 159-164
- M. G. Almzán-Torres, M. Jiménez-Reyes, F. Monroy-Guzmán, D. Tenorio, P. I. Aguirre-Martínez. 2004. Determination of the provenance of obsidian samples collected in the archaeological site of San Miguel Ixtapan, Mexico state, Mexico by means of neutron activation analysis. *J. Radioanal. Nucl. Chem.* 260(3): 533-542
- Map Center of China. The Statewide Chinese Map. Chinese Map Press, 2005
- Marek Lisiewicz, Robert Heimbürger, Jerzy Golimowski. 2000. Granulometry and the content of toxic and potentially toxic elements in vacuum-cleaner collected, indoor dusts of the city of Warsaw. *The Science of the Total Environment* 263: 69-78
- Nikolaos S. Thomaidis, Evangelos B. Bakeas, Panayotis A. Siskos. 2003. Characterization of lead, cadmium, arsenic and nickel in PM<sub>2.5</sub> particles in the Athens atmosphere, Greece. *Chemosphere* 52: 959-966
- Yingjun Liu, Liming Cao, Zhaolin Li, Henian Wang, Tongqing Chu, Jingrong Zhang. 1984. Elementary Geochemistry. Science Press: 65-377
- Z.G. Guo, J.L. Feng, Ming Fang, H.Y. Chen, K.H. Lau. 2004. The elemental and organic characteristics of PM<sub>2.5</sub> in Asian dust episodes in Qingdao, China, 2002. *Atmospheric Environment* 38: 909-919

# XRF 法快速测定铁钛精矿中 Fe、Ti 品位

郭生良 赖万昌 程锋 郭伟

(成都理工大学 核技术与自动化工程学院, 四川 成都 610059)

**[摘要]** 介绍了 XRF 法在快速测定铁钛精矿样中 Fe、Ti 品位中的应用, 用 IED2000P 型快速 X 荧光分析仪, 分析目标元素特征 X 射线计数率与含量的关系, 主要研究基体效应对测量结果的影响, 通过比较选用特散比与经验系数法相结合做三元回归计算的数理模型可较好的校正基体效应, 其分析结果相对误差在 0.2% 以内, 达到实际生产要求。

**[关键字]** X 射线荧光分析; 基体效应; 铁钛精矿

近年来, 随着新一代基于高分辨率电致冷半导体探测器 XRF 分析技术的研究与推广, 以新一代高分辨率 XRF 分析仪在同时快速测定铁钛矿中钛、铁的品位, 特别是高含量矿石样品的品位有着较好的效果。但在 XRF 分析中, 基体效应、密度效应、水分效应、不均匀效应等因素 (特别是基体效应) 会给元素含量分析带来影响。因此, 在激发源、测量装置逐步完善的前提下, 基体效应校正就成为取得可靠元素含量数据的关键。

为此, 笔者对 6 件铁钛精矿样品进行 XRF 分析提出了校正基体效应的数学模型, 使分析结果的相对误差在 0.2% 以内, 达到校正基体效应的目的。

## 1 测量仪器设备

选用  $^{238}\text{Pu}$  源和半导体探测器组合测量。采用的分析仪器是成都理工大学研制的 IED2000P 型 XRF 快速分析仪, 该仪器由探头、主机、电源、样杯 (附带) 等组成。探头采用 Si-PIN 电致冷半导体探测器, 探测器的面积为  $7\text{ mm}^2$ , 对  $5.9\text{ keV}$  的 X 射线的能量分辨率为  $190\text{ eV}$ 。同素激发源采用  $^{238}\text{Pu}$ 。

## 2 测量方法与工作过程

测量方法及操作步骤:

- (1) 用天平称 30 克左右样品放入样杯中, 并将样品用 20kg 力紧压使样品上下两个面平整, 特别是下面的面要尽量平整。
- (2) 开机后半小时待仪器稳定后, 选 100s 为一次测量时间开始测量。每件样品测量三次, 取平均值。
- (3) 记录下仪器显示的所测样品中 Fe、Ti 及反散射峰的计数率。

## 3 影响因素及校正模型

第一作者简介: 郭生良 (1981.10-), 男, 陕西西安人, 2005 年成都理工大学核工程与核技术专业本科毕业, 现为成都理工大学核技术与自动化工程学院核技术及应用专业硕士研究生。

### 3.1 影响因素分析

该批样品是经加工后的干燥均匀粉状物，测量是在压实后进行的，而且样品测量面平整。因此，不平整度影响、矿化不均匀性影响、水分影响、密度影响等不是主要的影响因素。在这种条件下，基体效应是主要影响因素。

### 3.2 基体效应讨论及对策

该批铁钛精矿的主要成分有：Ti(30~47%)和Fe(29~35%)还有 O、Si 、Mn、Ca 、Al 、S、K、Na 、Mg 等,它们的含量在28%~41%之间。

由于 Fe、Ti 含量较高，Ti 的吸收限能量又小于 Fe 的特征 X 射线荧光的能量，因此, 在 Fe、Ti 含量的高精度分析中,Fe 对 Ti 有较强的特征增强效应，Ti 对 Fe 有较强的特征吸收效应。

因而，在分析 Fe、Ti 含量时,基体效应主要是 Ti 对 Fe 的吸收效应、Fe 对 Ti 的特征增强效应、Mn 对 Fe 的干扰和其它元素的吸收效应。可采用特散比法与经验系数法相结合校正基体效应,即先以特散比法校正其它轻元素的吸收效应,再用经验系数法校正

Ti 对 Fe 的特征吸收效应。

结合特散比法与经验系数法所采用的校正模型及回归结果如下：

$$\text{Fe}\% = a + bR\text{Fe} + cRTi + dRMn \tag{1}$$

$$a = 19.64 \quad , \quad b = -0.1126$$

$$c = 2.633 \quad , \quad d = -0.3481$$

$$\text{Ti}\% = a + bR\text{Fe} + cRTi + dRMn \tag{2}$$

$$a = 44.12 \quad , \quad b = -2.357$$

$$c = 8.738 \quad , \quad d = -14.37$$

式中：Fe%、Ti%分别为 Fe、Ti 元素的含量；R 为目标元素的特征 X 射线计数率与激发源放出的初级射线在待测样品表面产生的散射射线计数率之比；a、b、c、d 均为经验系数。

## 4 结果分析与应用

XRF分析值与推荐值（化学分析结果）对比如表1所示。从表中可得：XRF分析的Fe含量最大绝对误差小于0.02%，最大相对误差小于0.058%，平均值绝对误差为0.012%，平均绝对误差为0.034%；分析的Ti含量最大绝对误差小于0.07%，最大相对误差小于0.182%，平均值绝对误差为0.056%，平均绝对误差 0.13%。

表 1 XRF 分析与推荐值对比表

Fe 含量推荐值	(1)式分析值	绝对误差	相对误差 %
34.38	34.36	0.02	0.058
33.83	33.83	0	0
34.64	34.66	0.02	0.058
29.25	29.24	0.01	0.034
29.32	29.33	0.01	0.034
平均值	32.28	0.012	0.037
Ti 含量推荐值	(2) 式分析值	绝对误差	相对误差 %
46.38	46.32	0.06	0.129
46.28	46.26	0.02	0.043
46.09	46.16	0.07	0.151
37.18表	37.12	0.06	0.161
38.31	38.38	0.07	0.182
平均值	42.85	0.056	0.131

由此可知, XRF分析铁钛精矿中Fe、Ti含量其准确度、精密度均符合推荐值(化学分析)的误差标准。达到校正基体效应的目的,可满足实际生产的需要。

将上述铁钛矿样作为标准样品来刻度IED-2000P XRF分析仪,就可以在相同测量条件下快速分析同类型铁钛矿的Fe、Ti 品位。

## 4 结束语

在铁钛精矿的XRF快速分析中,提出用特散比法和经验系数法相结合做三元线性回归的数学模型,不但公式简单运算速度快而且还可以较好的校正基体效应对元素含量的影响,使分析精度满足生产要求。

用该方法分析的样品刻度XRF分析仪,可快速检测铁钛矿石的品位,检测速度高(分析时间仅为100s)、高效、方便、分析精度大大提高,用于选矿领域有良好的经济效益。

### 参考文献

- [1] 葛良全,周四春,赖万昌编著 原位X辐射取样技术。成都:四川科学技术出版社,1997
- [2] 赖万昌,葛良全,吴建平,等 铁矿石XRF现场取样技术的研究与应用1 核技术,1995 (12):744~ 749
- [3] 肖刚毅,赖万昌,葛良全 应用XRF分析仪快速分析铁精矿中的Si、S、K和TFe 含量 物探与化探 2002 (4): 313~ 315
- [4] 赖万昌,EDXRF 法直接测定铁氧体中MnO、ZnO 和Fe<sub>2</sub>O<sub>3</sub> 的含量[J]. 核技术,1994,17 (9):531 - 534.
- [5] 赖万昌 葛良全 吴永鹏 肖刚毅 林延畅.轻便型XRF分析仪在铁精矿品质快速检测中的应用.金属矿山 2003 (7): 48~ 52

## XRF TECHNIQUE FOR RAPID DETERMINATION OF Fe .Ti. CONTENT OF Fe.Ti-METAL ORE CONCENTRATES

Guo Sheng-Liang Lai Wang-Chang Cheng Feng Guo Wei

(Chengdu University of Technology, Chengdou, 610059)

**[Abstract]** This paper deals with X-ray fluorescence technique for rapid determination of Fe、Ti content of Fe、Ti-metal ore concentrates. The analytical precision and accuracy of this technique are consistent with the chemical analytical error standard and can meet the practical production requirements.

Overcoming matrix effect is a key problem in XRF. The authors analyze the X-rays fluorescence counts and content of each element. On this basis, the equation of joint application of 'the ratio of characteristic to scatter and the correction of experience coefficient' is built to overcome matrix effect.

The detecting system is IED 200P which is consisted of a <sup>238</sup>Pu source, a Si-PIN electrical refrigeration semiconductor detector. Selecting 100s as a measure time.

**[Key words]** X-ray fluorescence analysis ; matrix effect ; Fe-Ti concentrate



# x- $\gamma$ 吸收剂量率检测仪显示电路的研究

崔 妍 侯新生

成都理工大学

**[摘要]** 本文阐述了 X、 $\gamma$  射线吸收剂量率测量显示的软件电路的实现, 采用以单片机和液晶显示器为核心的设计方案, 详尽介绍了其工作原理。程序采用 C 语言编写, 并给出了程序流程图及相应程序。其中, 数据处理部分, 在标定系数的基础上, 引入修正系数, 使其针对不同的测量对象能通过调整取值范围而适应相应的改变。另外, 液晶显示器的控制驱动以及与单片机的硬件接口, I<sup>2</sup>C 总线虚拟, 也是本文着重说明的部分。经实验证明, 该系统能满足对 X、 $\gamma$  射线的吸收剂量率进行实时处理和显示, 量程范围较宽。工作状态稳定, 可以应用在嵌入式系统中作为人机界面。

**[关键字]** 单片机; 液晶显示器; 接口; 吸收剂量率

在医疗、同位素操作、核技术应用等工作场所, 常需要对工作人员的辐射防护和环境污染程度进行 X— $\gamma$  射线的辐射剂量监测。目前国内外众多仪器都局限于针对单一种类 X 射线或  $\gamma$  射线进行测量, 且智能化程度不高。因此, 同时监测 X 射线和  $\gamma$  射线的吸收剂量率是本课题的最终目的。

本课题在 AT89C52 单片机及 1601 液晶显示模块的基础上, 完成硬件电路设计及软件的编程, 以实现单片机对液晶显示器的控制。具体所要完成的工作包括: 数字显示测量结果, 倒计时功能, 任意测量时间设定功能, 以及具备一定抗干扰能力, 误差范围控制在  $\pm 10\%$  以内。

## 1 总体设计方案

总体的设计主要是 LCD 的控制/驱动和外界的接口设计。控制主要是通过接口与外界通信、管理内/外显示 RAM, 控制驱动器, 分配显示数据; 驱动主要是根据控制器要求, 驱动 LCD 进行显示。控制器还常含有内部 ASCII 字符库。小规模的设计, 常选用一体化控制/驱动器; 中大规模的设计, 常选用若干个控制器、驱动器, 并外扩适当的显示 RAM、自制字符 RAM 或 ROM 字库。本系统为典型的实时控制系统, 易于用单片机控制来实现, 基于单片机对液晶显示器的间接控制方式, 提出以下方案:

单片机的 P0 口作为数据口, 与液晶显示器的八位数据线相连接, 其它如使能 E, 读写控制 RW, 寄存器 RS, 也分别与单片机的准双向 I/O 口 P2 口的 P2.0~P2.2 相连。

SDA (串行数据线) 及 SCL (串行时钟线) 两根线与 P1.5 及 P1.6 相连, 作为二线制总线。具体情况如图 1.1 所示。